Annual Progress Report for JFY 2009

March 22, 2010

CDF Experiment

Spokespersons
Japan F. Ukegawa (University of Tsukuba)
U.S.A. R. Roser (Fermilab) and J. Konigsberg (University of Florida)

The CDF experiment at the Fermilab Tevatron proton-antiproton collider continued to accumulate high-statistics data and produce rich physics results in 2009. The accelerator performance has been superb. The instantaneous luminosity at the beginning of stores consistently exceeds $\mathcal{L} = 3 \times 10^{32}$ cm^{-2} s^{-1}, with a record luminosity of 3.77×10^{32} cm^{-2} s^{-1} in March 2010 (Figure 1 (top)). A weekly integrated luminosity in excess of 60 pb^{-1} has also been achieved regularly. The integrated luminosity in the calendar year 2009 amounted to about 2 fb^{-1} despite a long shutdown in summer, and the Run II total to date has now exceeded 8 fb^{-1} (Figure 1 (bottom)).

The upgraded CDF detector has been operational very successfully with high efficiency. The integrated luminosity recorded by CDF amounts to 6.8 fb^{-1}, roughly 62 times that of Run I (Figure 2). CDF expects to collect a total of about 7.8 fb^{-1} at the end of US fiscal year 2010, and close to 10 fb^{-1} by the end of 2011 if the Tevatron running continues. The CDF detector has been operating reliably, and it resulted in high efficiency in data taking.

CDF has analyzed up to 5.4 fb^{-1} of data thus far, depending on data sets and physics topics, and many important and interesting results have emerged. In this report we summarize these physics results, with an emphasis on contributions from the Japan group.

1 Physics Results

1.1 Top quark physics

The top quark and its properties have been studied extensively since its discovery by CDF in 1995. With increased statistics of Run-II data, these studies are now performed with high precision.

The top quark analyses with Run-II data include measurements of the mass and production cross section using various decay channels.

The top quark mass is extracted using various techniques and channels. By combining all measurements, CDF finds the top quark mass to be $m_t = 172.6 \pm 0.9 \pm 1.2$ GeV/c^2. The precision has long surpassed the original Run-II (2 fb^{-1}) goal of 3 GeV/c^2 and is now better than 1%. Using also the measurements by the D0 experiment, we derive the combined top quark mass of $m_t = 173.1 \pm 0.6 \pm 1.1$ GeV/c^2 (March 2009).

A measurement of the W boson mass has been performed by CDF. Combining it with top quark mass measurements provides indirect information on the Higgs boson mass through electroweak radiative corrections. Figure 3 shows the results as of August 2009. A constraint on the standard model Higgs boson mass is obtained to be $83\,^{+30}_{-23}$ GeV/c^2 at 68% CL, and is less than 154 GeV/c^2 at 95% CL (Figure 4).

Other production and decay properties of the top quark are also studied, including $t\bar{t}$ spin correlations at production and the $W^{\pm}$ boson helicity in the decay.

The top quark should have a decay width of about 1.3 GeV in the Standard Model, corresponding to a lifetime of about 10^{-24} s. The time is shorter than the hadronization scale, therefore the top quark is expected to decay as a free quark instead of quarks in hadrons. Coupled with the fact that the charged weak interaction violates parity, it means that the decay products of the top quark, for example the charged lepton from the W boson, carry information about the spin of the parent top quark.

It would be impossible to measure the lifetime directly, but the correlations in the spin states of $t\bar{t}$ pairs can be observed, given that the pairs are produced at Tevatron mainly through the subprocess $q\bar{q} \to t\bar{t}$, which is governed by the vector-type strong interaction couplings.

Y. Takeuchi (Tsukuba) has measured $t\bar{t}$ spin correlations using the di-lepton channel of the top quark pair events. The angle is measured between the charged lepton flight direction in the top quark rest frame and an appropriately chosen axis of spin quantization. The two-dimensional distribution of the angles for positive and negative leptons is examined. The distribution in general has a form

$$\frac{1}{N}\frac{d^2N}{d\cos\theta_+\, d\cos\theta_-} = \frac{1+\kappa\cos\theta_+\cos\theta_-}{4},$$

where κ is the parameter representing the degree of correlation. For the subprocess $q\bar{q} \to t\bar{t}$, it is expected that $\kappa = +1$. The expected distributions for $\kappa = +1$ before and after inclusion of the detector acceptance are shown in Figure 5. The real data angular distribution (2.8 fb^{-1}) and the log-likelihood distribtuin for κ are shown in Figure 6. Using the Feldman-Cousins method, the parameter κ is determined to be $\kappa = +0.320\,^{+0.545}_{-0.775}$ [1], consistent with the Standard model prediction of $\kappa \simeq +0.8$.

1.2 Bottom quark physics

Since the 2006 observation of the particle-antiparticle oscillations of the B_s^0 meson and a measurement of their frequency Δm_s, CDF has turned its attention to more detailed studies

of B-hadron decays and searches for possible new effects originationg from physics beyond the Standard Model and the CKM theory.

For example, we have looked for CP violation in B_s^0-$\bar{B}_s^0$ mixing, which modulates with the frequency Δm_s. The decay mode $B_s^0 \to J/\psi\,\phi$ is the most useful for this purpose. A measurement based on a 2.8 fb^{-1} dataset is published, and we have obtained the first constraint on the phase β_s and already eliminated a wide range of the parameter space. An update using a 5.2 fb^{-1} dataset is under way and will soon be made public.

Another interesting field of study is the B-hadron decays proceeding by the FCNC processes $b \to s$. H. Miyake (Tsukuba) has observed signals for $B^+ \to K^+\,\mu^+\mu^-$, $B_d^0 \to K^{*0}\,\mu^+\mu^-$, and $B_s^0 \to \phi\,\mu^+\mu^-$ (Figure 7). The last mode is the first observation of the mode, and represents the most rare decay mode ever for the B_s^0 meson. The muon pair invariant mass distributions are examined, and the corresponding differential branching fractions are determined. Interesting observables in these decays are the polarization and the the lepton angle forward-backward asymmetry. The Standard Model processes have both vector and axial-vector couplings in thoese decays, and therefore an asymmetry is expected to be non-zero and has been observed in previous measurements. However, the existence of new physics could change drastically those distributions, and a hist of possible effects has been observed by the Bell experiment. The distributions are shown in Figure 8 [2]. The asymmetry distribution follows the trend of the Belle measurement, and remains to be an important subject to be checked with higher statistics.

1.3 New particle searches

Searches for the Higgs boson, supersymmetric particles and other new particles have been performed. Cross sections for the standard model Higgs boson production at the Tevatron is shown in Figure 9 (left) for various subprocesses. The largest contribution comes from the single production through gluon fusion, with the top quark in the loop. Associated production with a weak boson, $W^{\pm}H$ and Z^0H, is smaller. The decay branching fractions of the Higgs boson are shown in Figure 9 (right). At a low mass, below 135 GeV/c^2, the decay to $b\bar{b}$ pairs is dominant, while at a high mass the decays to weak boson pairs become dominant.

CDF has searched for the Higgs boson production using many different final states. The first, aimed at a low mass Higgs, looks for the associated production $\bar{p}p \to VHX$, where V is a weak gauge boson $W^{\pm}$ or Z^0, with the $W^{\pm}$ (Z^0) boson decaying into $\ell^{\pm}\nu$ ($\ell^+\ell^-$, $\nu\bar{\nu}$) pairs, and the Higgs boson to $b\bar{b}$ pairs. The b quark jets are identified with displaced vertices. The main background comes from heavy flavor ($b\bar{b}$, $c\bar{c}$) production in association with the vector boson V, and top quark pair production. Various kinematic distributions, including the di-jet mass distribution (Figure 10 (left)), are examined for possible production of the Higgs boson. Also an artificial neural network discriminant is employed (Figure 10 (right)). No excess of events over known backgrounds is found in 4.3 fb^{-1} of data, and upper limits on

the Higgs boson production cross section are set, in the range of 4.0 to 38 times the standard model value, depending on the assumed Higgs boson mass (110 to 150 GeV/c^2) [3]. Y. Nagai (Tsukuba) has performed the analysis and extended the search using the electrons produced in the endplug region. M. Kurata (Tsukuba) is applying the Dynamical Likelihood Method to the Higgs search in this channel.

The second analysis looks for single production of the Higgs boson followed by its decays to W boson pairs. The channel is sensitive to a high mass Higgs. The W^+W^- final state is identified with their decays to leptons, thus the signature is two energetic leptons and a large missing transverse energy and nothing else. The dominant background comes from electroweak W^+W^- production, which leads to the same signature. However, there exists a difference in event topology, for example the lepton azimuthal angle correlations. Again, no excess of events is observed and upper limits on Higgs production have been placed. This is presently the most sensitive search channel at CDF, and the upper limit for the mass of 165 GeV/c^2 is 1.23 times the Standard Model values.

The third method looks for associated production of the Higgs boson with a weak boson $W^\pm$ or Z^0, where the Higgs boson decays to W^+W^- boson pair and one or both of the W boson can be off mass shell. There exist three weak bosons in the final state, where two of them have the same charge. They are required to decay leptonically, leading to a very distinctive final state of isolated, same-charge lepton pairs, such as $e^+\mu^+$.

The results from different analyses are combined and summarized in Figure 11, where the ratio of the obtained upper limits on production cross sections to the standard model predictions is presented. The limits are at a factor of 1.2 for a Higgs mass near 160 GeV/c^2, and are 2.5 to 3 times the SM value at low mass [4]. Figure 12 shows the limits where the results from both CDF and D0 experiments are combined. Data up to 5.4 fb^{-1} have been analyzed. A mass range between 163 GeV/c^2 and 166 GeV/c^2 has been excluded at 95% CL [5].

References

[1] "Measurement of the $t\bar{t}$ spin correlations in 2.8 fb^{-1} dilepton candidates",
CDF Collaboration, CDF public note 9824 (2009).

[2] "Measurement of forward-backward asymmetry in $B \to K^{(*)}\mu^+\mu^-$ and search for $B_s^0 \to \phi\mu^+\mu^-$",
CDF Collaboration, CDF public note 10047 (2010).

[3] "Search for standard model Higgs boson production in association with a $W^\pm$ boson using neural netwrks with 4.3 fb^{-1} of CDF data",
CDF Collaboration, CDF public note 9997 (2009).
"Search for the Standard Model Higgs Boson in the $WH \to \ell\nu b\bar{b}$ Channel in 1.96-TeV

Proton-Antiproton Collisions",
Yoshikazu Nagai, Ph. D. Thesis, University of Tsukuba, February 2010.

[4] "Combined upper limit on standard model Higgs boson production at CDF for HCP 2009",
CDF Collaboration, CDF public note 9999 (2009).

[5] "Combined CDF and D0 upper limits on standard model Higgs-boson production with 2.1 - 5.4 fb^{-1} of data",
CDF and D0 Collaborations, arXiv:0911.3930 [hep-ex] (2009).

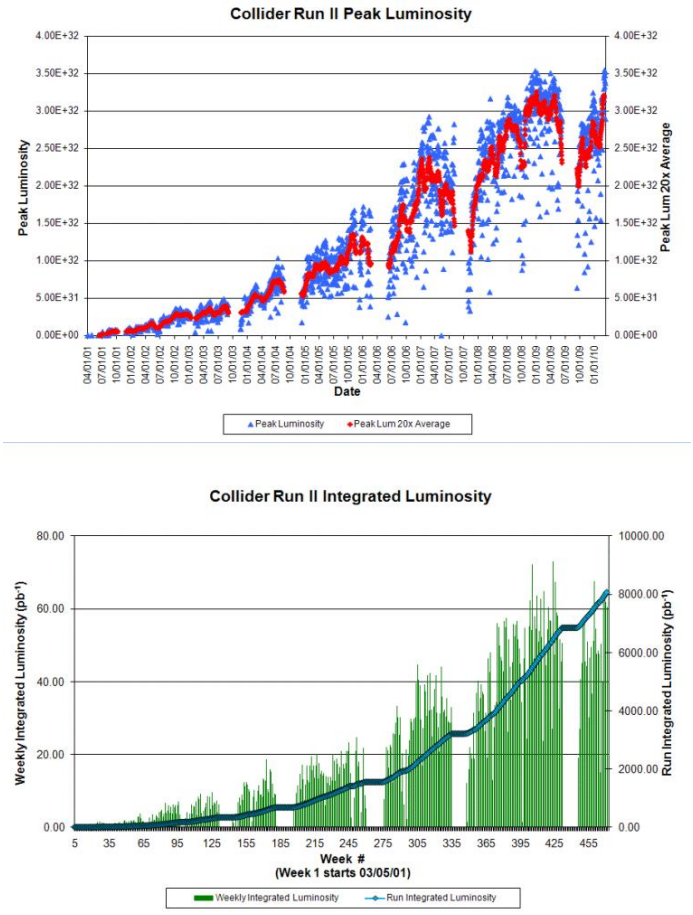

Figure 1: Tevatron performance in Run II. Top: instantaneous luminosity at the beginning of each store. Bottom: integrated luminosity delivered by week.

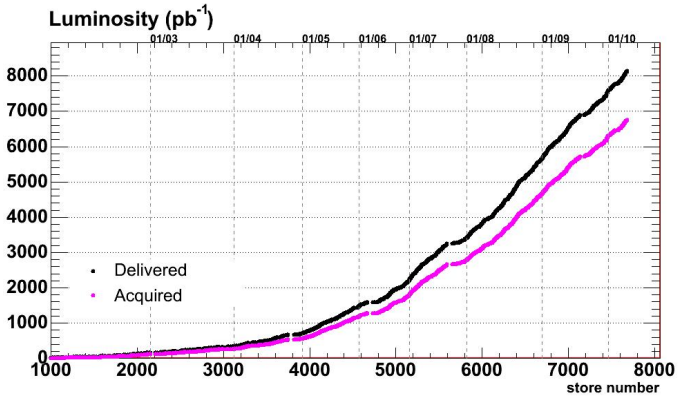

Figure 2: Integrated luminosity (top) delivered to and (bottom) recorded by CDF in Tevatron Run II.

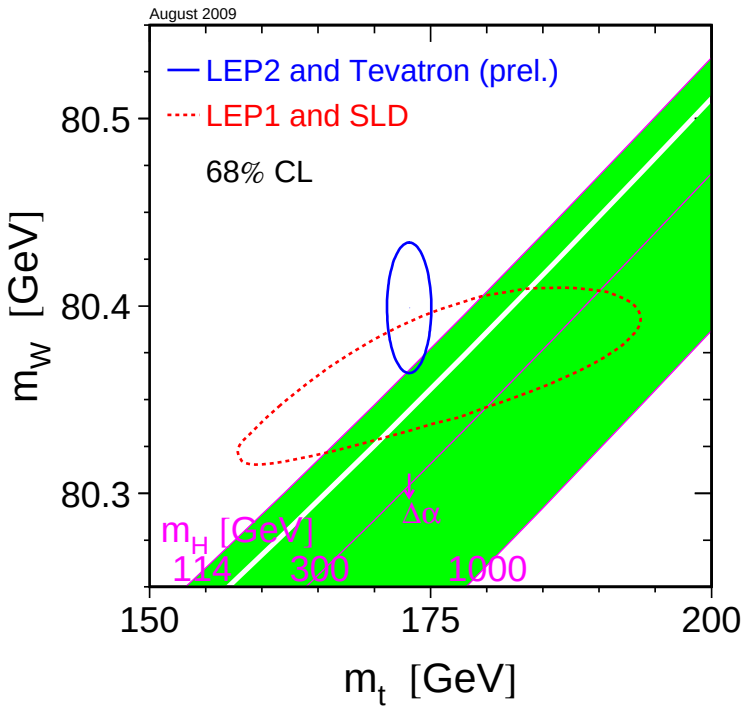

Figure 3: Measurements of the top quark and W boson masses as of August 2009, and indirect information on the Higgs boson mass.

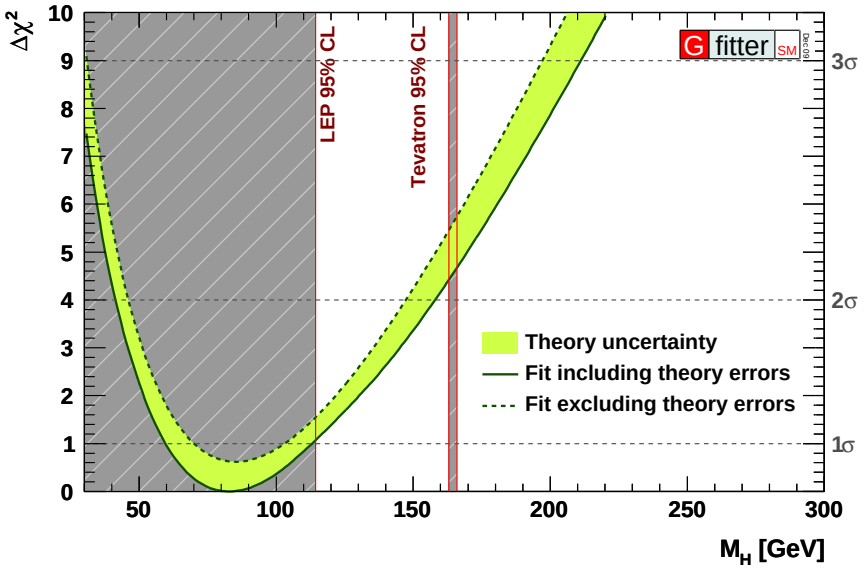

Figure 4: Likelihood distribution for the Higgs boson mass derived from global fits to electroweak measurements.

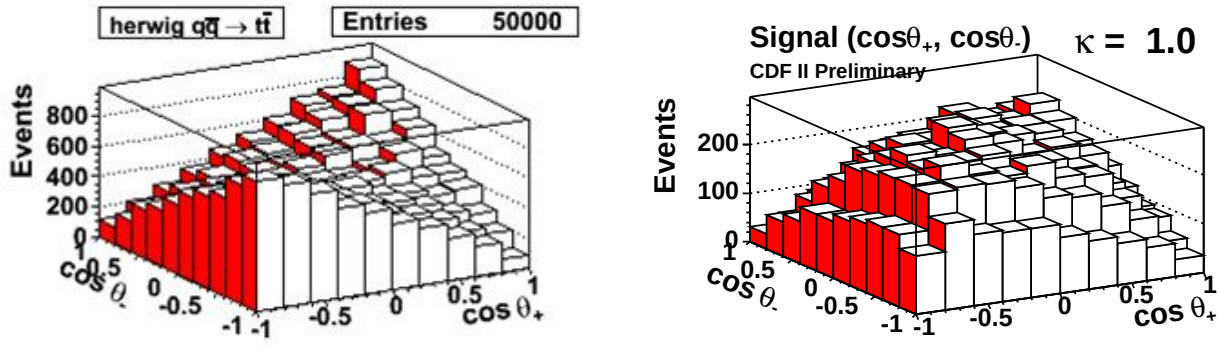

Figure 5: Study of spin correlations in $t\bar{t}$ production. Two-dimensional distributions of the positive and negative lepton angles expected for the subprocess $q\bar{q} \to t\bar{t}$, before and after inclusion of the detector acceptance.

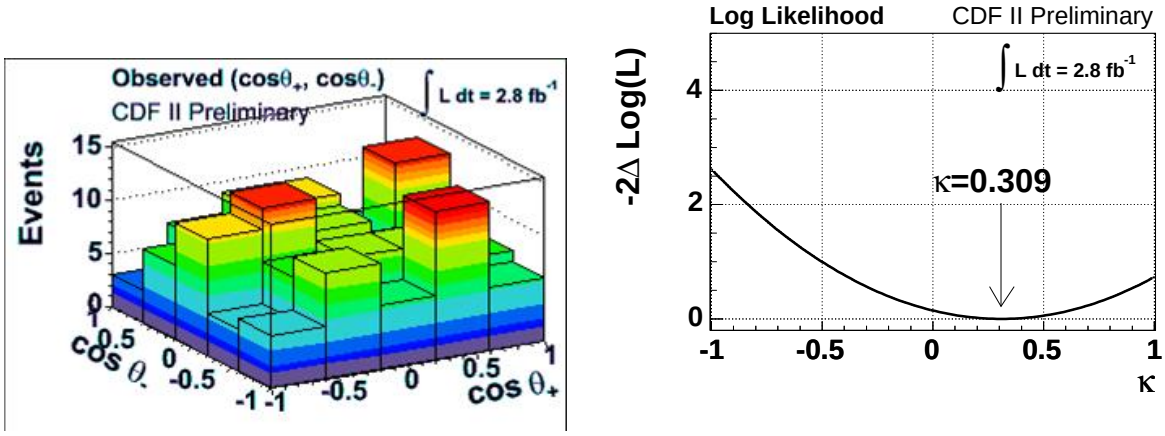

Figure 6: Study of spin correlations in $t\bar{t}$ production. Left: real data angular distribution. Right: Log-likelihood distribution for the parameter κ.

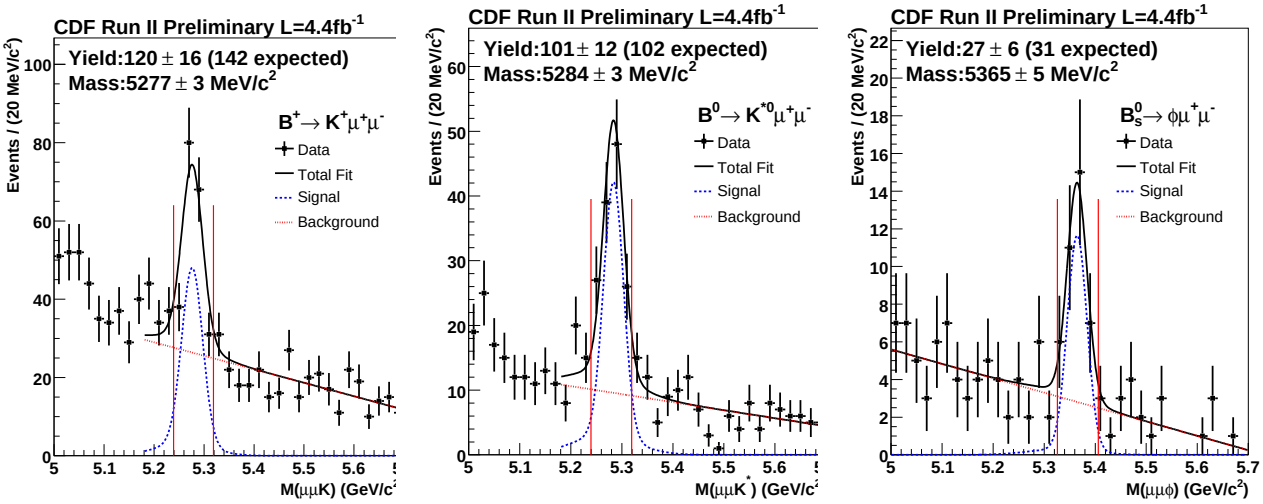

Figure 7: Signals for $B^+ \to K^+ \mu^+\mu^-$, $B_d^0 \to K^{*0} \mu^+\mu^-$, and $B_s^0 \to \phi \mu^+\mu^-$.

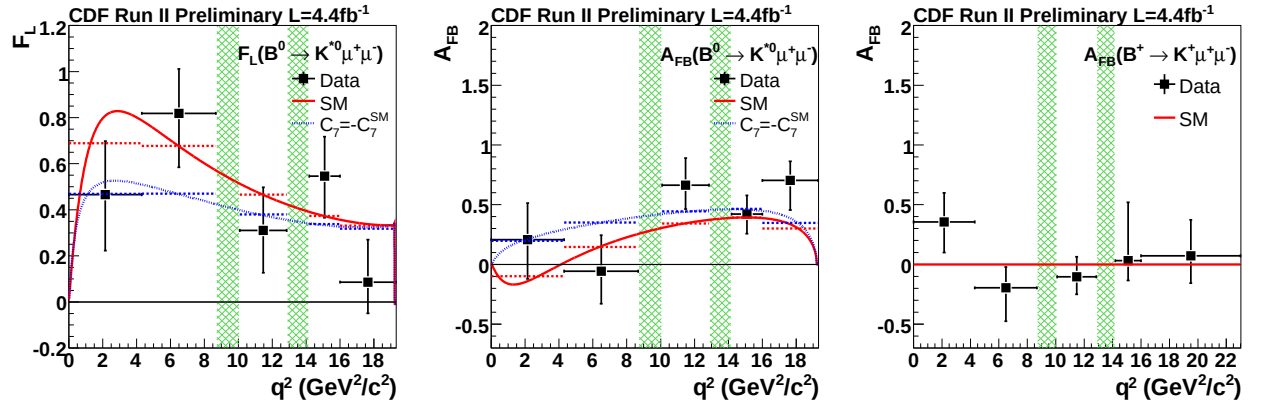

Figure 8: Left and center: Polarization and lepton forward-backward asymmetry for the decay $B_d^0 \to K^{*0} \mu^+\mu^-$. Right: Lepton forward-backward asymmetry for the decay $B^+ \to K^+ \mu^+\mu^-$. All distributions are shown as a function of the $\mu^+\mu^-$ mass-squared.

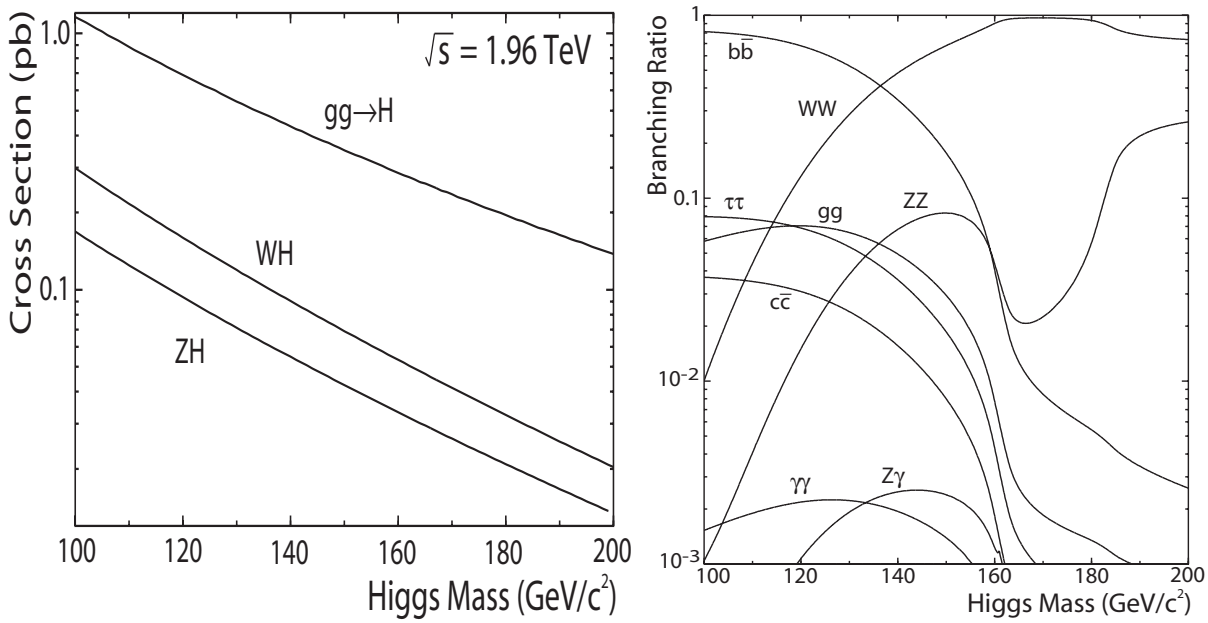

Figure 9: Left: Cross section for the production of the standard model Higgs boson at Tevatron. right: Branching fractions of the standard model Higgs boson to various final states. Both plots show dependences on the Higgs boson mass.

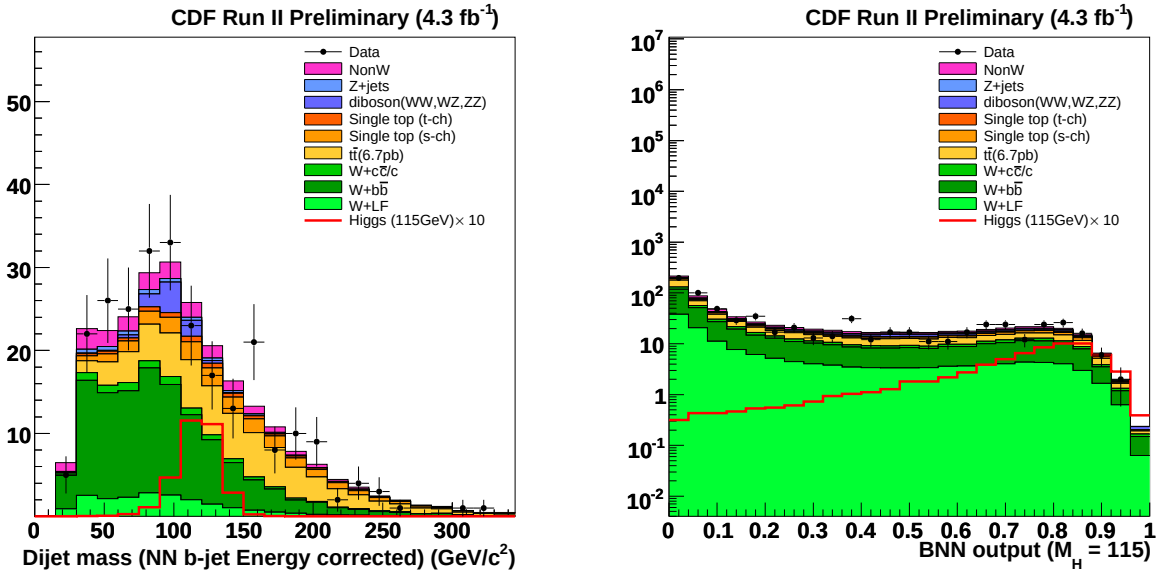

Figure 10: Higgs boson search in the $p\bar{p} \to W^{\pm}HX \to (\ell^{\pm}\nu)\,(b\bar{b})\,X$ channel. Left: Invariant mass distribution of the two b-quark candidate jets produced in association with a W boson. Right: Output of the Bayesian neural network discriminant.

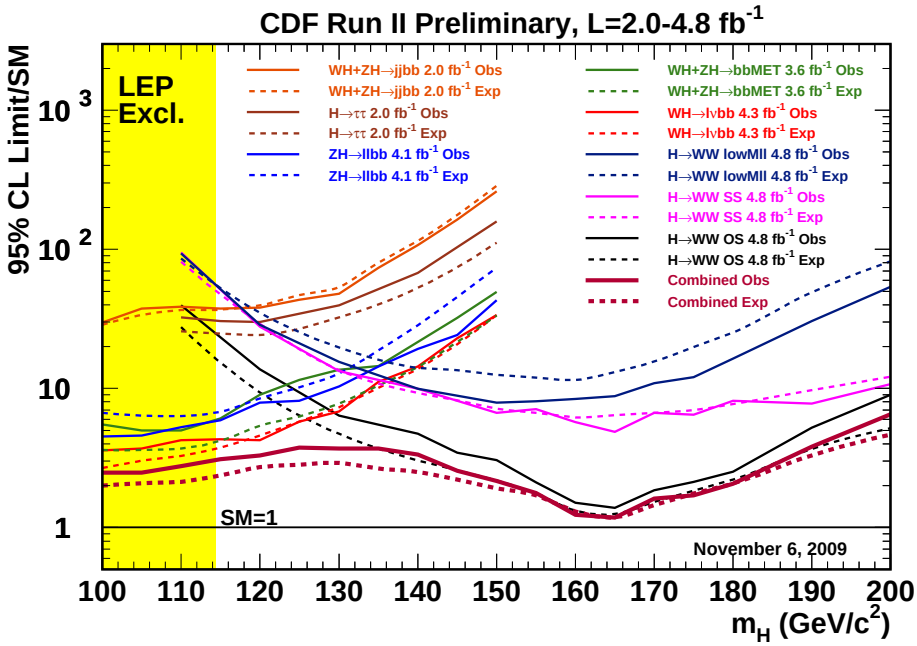

Figure 11: Summary of CDF results on the searches for the standard model Higgs boson. The experimental upper limits on production cross sections, normalized to the theoretical predictions, are shown for all search channels.

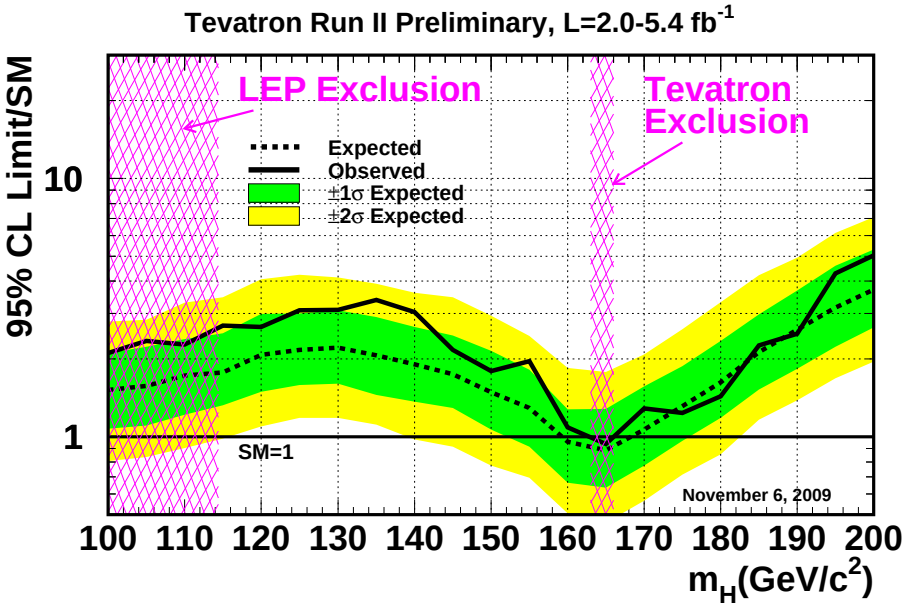

Figure 12: Summary of combined CDF and D0 results on the searches for the standard model Higgs boson. The experimental upper limits on production cross sections, normalized to the theoretical predictions, are shown after combining all search channels. The mass range between 163 GeV/c^2 and 166 GeV/c^2 has been excluded at 95% CL.